The Chemistry in Air of the Rare-earth-metal Sesquioxides. Comparative Study of Hexagonal and Cubic Neodymia Samples

Serafín Bernal,* Francisco J. Botana, Rafael García, and José M. Rodríguez-Izquierdo
Departamento de Química Inorgánica, Facultad de Ciencias, Universidad de Cádiz, Apartado 40, Puerto Real, 11510 Cádiz, Spain

The evolution in air of four different neodymia samples, two of them with hexagonal structure and the other two cubic, has been studied. Upon exposure to air the four samples become heavily hydrated. Likewise, carbonation, though much less intense, does affect the bulk oxides. The behaviour of the hexagonal samples on the one hand, and that of the cubic oxides on the other, was found to be quite different. Dissimilarities were observed in the rates of the aging processes, being much faster for the cubic oxides, in the nature of the carbonated phases, and in the thermal evolution of samples stabilized in air. In the case of the cubic neodymium oxides, a crystalline carbonate hydroxide-like phase, isostructural with that observed for cubic samaria and europia samples aged in air, was found. By contrast, the carbonated phase of the hexagonal neodymias seems to be similar to those detected for hexagonal lanthana, as well as for a monoclinic sample of samaria. The results, in addition to showing that the behaviour in air of the rare-earth-metal oxides is much more complex than presumed earlier, give further support to the tentative classification of these oxides into three groups.

The rare-earth-metal oxides are used as starting materials to prepare novel phases like superconducting ceramics[1] and catalysts,[2] currently of great interest. As a consequence, it has become apparent that there is a lack of detailed information about several aspects of the chemistry of lanthanide oxides, the knowledge of which is essential to interpret their behaviour, and to develop their technological applications.

One aspect worthy of further investigation is the reactivity of the 4*f* sesquioxides to atmospheric CO_2 and H_2O, at ordinary temperature and pressure,[3] *i.e.* under the usual storage and manipulation conditions. As we have shown,[4–6] aging may have profound effects on both the mechanism and the actual nature of the phases resulting from reactions involving lanthanide oxides. Studies specifically concerned with aging of rare-earth-metal oxides in air are, however, very scarce, which prompted us to initiate a research project on this topic[7–13] the results of which have recently been reviewed.[14]

According to our earlier investigations on samaria,[11–13] not only the intensity of the aging processes but also the structural nature of the resulting phases can be very different for samples of the same 4*f* sesquioxide. Such differences might well be related to the structural nature, either cubic or monoclinic, of the starting samarium oxides.

Since neodymia can exhibit at ordinary temperature and pressure the hexagonal (A) and cubic (C) structures of Ln_2O_3,[15] this oxide constitutes a good candidate to investigate further the relationship between structure and reactivity to atmospheric H_2O and CO_2. In the present work, results corresponding to four different neodymium oxides are reported. Two of these samples showed the hexagonal structure, and the other two the cubic one. The study includes the characterization of the starting oxides as well as of the final aged-in-air phases. The evolution of the samples throughout the whole aging process was also investigated. Finally, the mechanism of the thermal decomposition of the aged phases was studied and is discussed.

Experimental

Data corresponding to the preparation of the four neodymia samples investigated in the present work, hereafter referred to as A1, A2, C1, and C2, are summarized in Table 1.

The hydroxide nitrate was precipitated from an aqueous solution of $Nd(NO_3)_3 \cdot 6H_2O$, 99.9% pure (Fluka), with a large excess of aqueous concentrated ammonia (Merck). The precipitate was washed with distilled water and dried in a flow of helium at 383 K.

The starting $Nd(OH)_3$ used to prepare sample C2 was obtained by rehydrating an oxide obtained from the calcination in a flow of He, at 1 273 K, of an aged-in-air neodymia. The rehydration was carried out in a flow of He which had previously been bubbled through distilled water. The temperature was 350 K and the duration 24 h.

Thermogravimetry (t.g.) experiments were carried out with a Mettler model ME-21 microbalance. The flow rate of He was 1 $cm^3\ s^{-1}$, and the heating rate 0.1 $K\ s^{-1}$.

The temperature-programmed decomposition (t.p.d.) experi-

Table 1. Data on the preparation of the neodymia samples investigated

Sample	Neodymia precursor	Flowing gas	Heating rate/K s^{-1}	Calcination temperature/K	Calcination time/h
A1	Nitrate hydroxide	He	0.15	1 020	4.0
A2	Nitrate hydroxide	He	0.15	1 310	3.0
C1	Nitrate	H_2	0.03	770	0.2
C2	Hydroxide	H_2	0.15	820	0.1

Table 2. Aging in air of the hexagonal and cubic neodymia samples

	Starting oxides		Aging process: total weight gain (%) upon exposure to air						Stabilized in air samples *			
Sample	Crystallite size/nm	$S_{BET}/m^2\ g^{-1}$	1	5	10	20	30	50 d	H_2O (%)	CO_2 (%)	Crystallite size/nm	$S_{BET}/m^2\ g^{-1}$
A1	89	6.4	0	0	11	38	63	96	15.0 (289)	2.5 (20)	32	14.8
A2	118	2.2	0	0	0	11	61	99	15.3 (389)	2.2 (23)	24	11.2
C1	30	5.0	28	79	88	96	100	100	12.4 (696)	2.2 (50)	22	5.2
C2	36	17.4	42	68	75	82	98	100	12.3 (226)	2.8 (21)	22	15.8

* Values in parentheses are the numbers of molecules per nm^2.

ments were performed under the following conditions: flow rate of He, 1 $cm^3\ s^{-1}$; heating rate, 0.1 K s^{-1}. The gases evolved were analysed by mass spectrometry (m.s.), with a VG model Spectralab SX-200 instrument.

The i.r. spectra were recorded either with a Nicolet model 5 DXE Fourier-transform instrument or a conventional Perkin-Elmer model 710 B spectrometer. The discs containing 5% of the sample and 95% of KBr were pressed into wafers under a pressure of 5×10^5 kPa.

The *X*-ray powder diffraction diagrams were obtained with a Siemens model D-500 diffractometer, using zirconium-filtered Mo-K_α or nickel-filtered Cu-K_α radiation. The mean crystallite sizes reported in this work were determined by applying the Scherrer equation for widening of the powder diffraction lines. Peaks corresponding to structures A and C of Nd_2O_3 as well as to $Nd(OH)_3$ appearing at around 0.220 nm were used. The instrumental widening was estimated from the diffraction pattern recorded for a gold sheet.

Results

The four neodymia samples were exposed to air at ordinary temperature and pressure, and their evolution systematically investigated by i.r. spectroscopy, *X*-ray powder diffraction, t.g., and t.p.d.–m.s. Also, the BET surface areas of both the starting oxides and the aged-in-air samples were determined.

Table 2 summarizes some of the results of our study. The two hexagonal oxides, A1 and A2, stabilized after approximately 50 d. In both cases an induction period of several days can be noted. The aging of the cubic samples C1 and C2 was much faster, occurring with no induction period. The amounts of water uptaken by the oxides roughly correspond to the complete transformation of Nd_2O_3 to $Nd(OH)_3$, *i.e.* 16%, which would indicate substantial hydration of the four samples. The carbonation is much less intense; however, if it is recalled that a monolayer of either H_2O or CO_2 adsorbed on 4*f* sesquioxides should not exceed 8 molecules per nm^2,[7,16] it can be concluded from the results in Table 2 that both the hydration and carbonation reactions affect the bulk of the four neodymia samples. The occurrence of bulk carbonation is particularly noteworthy because in some earlier papers dealing with the aging of neodymium oxides in air this process has been completely ignored.[17–19] In another case[20] the carbonation reaction is assumed to occur, but considered to be a surface process.

The evolution in air of the hexagonal neodymia samples is, as deduced from the i.r. spectroscopic study, similar to that reported for La_2O_3,[10] the only difference being the rate of the process, being much faster in the case of lanthana. This analogy

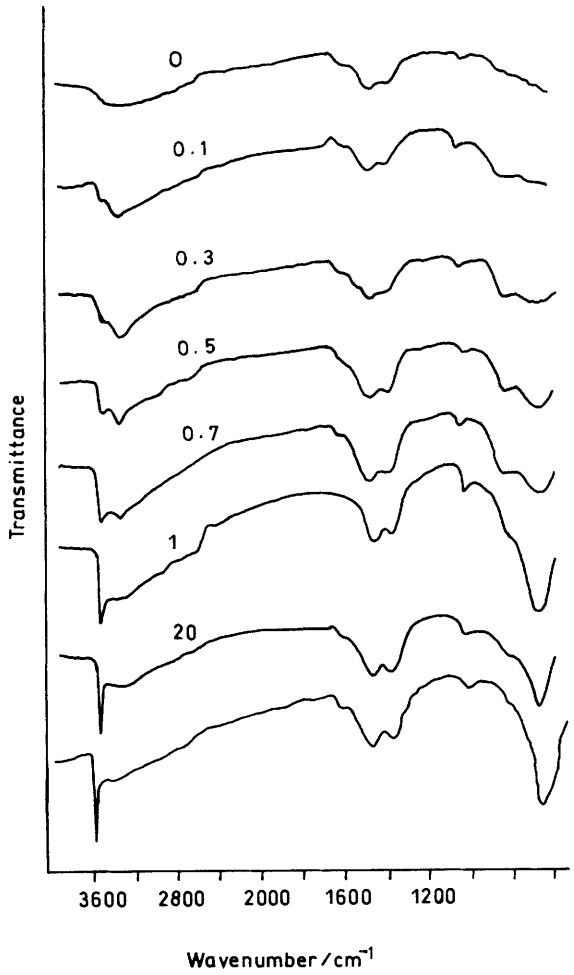

Figure 1. I.r. spectra for the evolution of sample C2 in air. The exposure time in days is indicated. The spectrum of the sample A2 stabilized in air (60 d) is shown at the bottom

means that the i.r. spectrum recorded at different stages of the process remains unchanged, so that we have included in Figure 1 only the spectrum of the stabilized oxide. The most remarkable features of this spectrum are the sharp band at 3 600 cm^{-1}, characteristic of rare-earth-metal hydroxides,[14,21,22] the strong band at 660 cm^{-1}, which can also be assigned to

Table 3. *X*-Ray powder diffraction data for the evolution of sample A2 in air

		Exposure time/d						
d/Å	Nd_2O_3 (A)*	10	20	28	34	48	60	$Nd(OH)_3$*
5.57	—	—	w	s	vs	vs	vs	vs
3.30	m	m	m	m	w	—	—	—
3.20	—	—	w	m	s	s	s	s
3.08	—	—	w	m	s	vs	vs	vs
2.99	m	m	m	m	w	—	—	—
2.90	vs	vs	vs	vs	s	m	—	—
2.77	—	—	—	vw	w	w	w	w
2.21	m	m	m	s	s	s	s	vs
1.91	m	m	m	m	w	—	—	—
1.85	—	—	vw	w	m	m	m	m
1.84	—	—	w	m	s	s	s	vs
1.71	m	m	m	m	w	—	—	—

w = Weak, m = medium, s = strong, and v = very. * Data from ASTM file.

Table 4. *X*-Ray powder diffraction data for the evolution of sample C2 in air

		Exposure time/d						
d/Å	Nd_2O_3 (C)*	0	0.2	0.4	0.6	1.0	60	$Nd(OH)_3$*
5.57	—	—	—	—	m	vs	vs	vs
4.00	—	—	vw	w	—	—	—	—
3.26	—	—	m	vs	vs	sh	sh	—
3.20	vs	vs	vs	vs	s	s	s	s
3.08	—	—	—	—	m	vs	vs	vs
2.83	—	—	w	m	w	vw	vw	—
2.77	s	s	m	w	w	w	w	w
2.21	—	—	—	—	m	s	s	vs
2.00	—	—	w	m	—	—	—	—
1.95	s	s	m	w	—	—	—	—
1.85	—	—	—	—	vw	m	m	m
1.84	—	—	—	—	w	s	s	vs
1.72	—	—	w	m	—	—	—	—
1.67	s	s	m	w	—	—	—	—

sh = Shoulder. * Data from ASTM file.

hydroxide,[14,23] and the two bands in the region 1 300—1 600 cm^{-1}, typical of carbonate species.

The spectra of cubic oxides stabilized in air are indistinguishable from those of samples A. Nevertheless, it is obvious from Figure 1 that the first stages of their aging lead to the formation of a phase other than that formed on the hexagonal neodymias. For the shortest exposure times, in effect, the spectrum of sample C2 is characterized by the absence of the band at 660 cm^{-1}, and the existence in the O–H stretching range of two bands at 3 600 and 3 425 cm^{-1}, the latter being the most intense. Also, absorptions due to carbonate species can be noted. This spectrum is similar to those reported by us for cubic samaria[11,12] and europia[14] stabilized in air which were assigned to a carbonate hydroxide-like phase.[12,14]

The further evolution of the spectrum of sample C2 exposed to air (Figure 1) suggests that the initial step is followed by the formation of $Nd(OH)_3$, as deduced from the growth of the band at 3 600 cm^{-1}, and the appearance of a strong feature at 660 cm^{-1}.

Tables 3 and 4 report the results of our *X*-ray powder diffraction study of the stabilization of the neodymium oxides in air. The diffraction patterns obtained for samples A can always be interpreted as due to oxide, hydroxide, or to the coexistence of both, Table 3. No diffraction lines suggesting the occurrence of any carbonated phase could be observed at any stage of the stabilization. This evolution pattern parallels that for La_2O_3 reported by us.[10,14]

Samples C1 and C2 behave very similarly to each other. At the very beginning of the process there are two diffraction lines at 0.326 and 0.283 nm which do not correspond to any of the phases described in the ASTM file for the ternary system Nd_2O_3–H_2O–CO_2. At this stage no hydroxide is formed, as deduced from the absence of the line at 0.557 nm. For exposure times longer than 1 d, the cubic oxide, the hydroxide, and the unidentified phase coexist. Finally, upon stabilization, the pattern essentially corresponds to that of $Nd(OH)_3$. However, the phase formed in the first stages of the process is also present, evidenced by the lines at 0.326 and 0.283 nm.

The stabilization of the four neodymium oxides in air was also investigated systematically by t.g. and t.p.d.–m.s., yielding the results in Table 2. Figure 2 depicts representative t.g. diagrams of hexagonal and cubic oxide samples aged in air. The differences between the two traces are notable, which suggests that t.g. may constitute a simple and useful technique to establish the structural nature of the starting neodymium oxides.

As in the case of the i.r. and *X*-ray powder diffraction results, the diagram in Figure 2 for sample A2 is similar to that of hexagonal lanthana aged in air,[10] a commercial sample of hexagonal neodymia,[14] as well as some monoclinic samarium oxides.[11,13] The i.r. spectra and powder diffraction pattern of the phases formed after each of the steps of decomposition of lanthana[10] aged in air allowed us to propose a mechanism for the process, which might well be applied to the present case. The first two

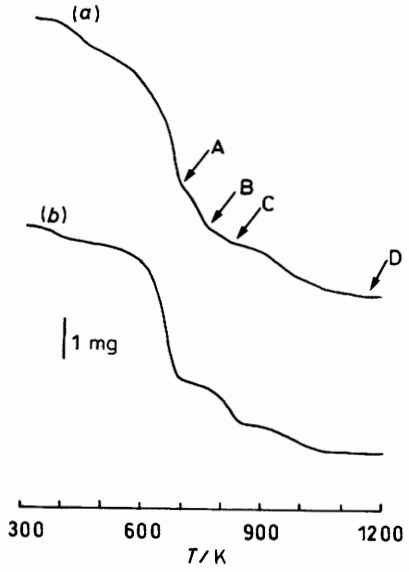

Figure 2. T.g. diagrams for samples C2 (*a*) and A2 (*b*) stabilized in air. The initial weight of the samples is indicated on the right-hand side. The arrows in (*a*) indicate the stages at which the decomposition process was stopped and the resulting phases investigated

weight losses in the t.g. diagram represent the dehydration of $Ln(OH)_3$ to the oxide through an intermediate hydroxide oxide, LnO(OH). The third step, corresponding to the evolution of CO_2, is interpreted as due to the decomposition of a monocarbonate dioxide phase, $Ln_2O_2(CO_3)$, to Ln_2O_3; the carbonate phase above arises from the decomposition of a carbonate hydroxide like phase ocurring through the first of the two steps of the dehydration reaction.

To gain information about the mechanism of the thermal decomposition of the cubic neodymium oxides aged in air, we have investigated by i.r. spectroscopy and powder diffraction the phases resulting from the successive steps of the process. The arrows in Figure 2 indicate the stages of the thermal decomposition at which the process was stopped and the resulting phases studied.

Figure 3 shows the i.r. spectra corresponding to the intermediate phases mentioned above. For comparison it also includes the spectrum of the oxide stabilized in air. Step A induces a notable decrease in intensity of the band at 3 600 cm^{-1}, as well as the disappearance of that at 660 cm^{-1}, both characteristic of $Nd(OH)_3$. Since this step also causes the complete elimination of the lines due to hydroxide in the powder diffraction pattern (Table 5), it is concluded that this first step corresponds to the decomposition of the hydroxide phase present in the aged sample. This is also consistent with the evolution of water detected in this step by t.p.d.–m.s.

Contrary to what was reported for the decomposition of hexagonal samples aged in air [8,10,20] no formation of NdO(OH) can be deduced from the powder diffraction pattern in Table 5. This suggests that in the case of the cubic neodymia samples the dehydration of the hydroxide occurs through a single step.

It is also worth noting that spectrum A in Figure 3 is similar to those obtained in the first stages of the aging of the cubic neodymium oxides in air, Figure 1. Likewise, it is analogous to those obtained for cubic samaria [11,12] and europia [14] exposed to air. The powder diffraction pattern of the phase resulting from step (*a*) is in accord with that observed at the initial stages of aging of the cubic oxides, Table 4, characterized by the lines at 0.326 and 0.283 nm.

In accordance with these i.r. and powder diffraction data, step

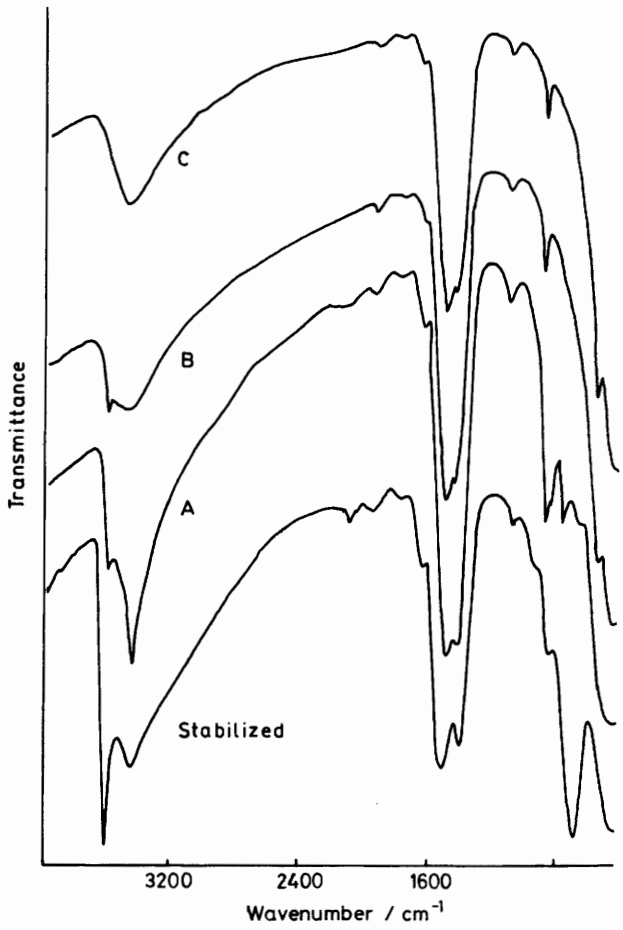

Figure 3. I.r. spectra of the phases resulting from freezing the decomposition of sample C2 aged in air at the stages marked with arrows on the t.g. diagram in Figure 2 (*a*)

Table 5. *X*-Ray powder diffraction data for the phases resulting from freezing the decomposition of sample C2 stabilized in air at the stages marked with arrows in Figure 2. Pattern A′ corresponds to the phase obtained by decomposition of aged C2 at 20 K above the temperature at which step A was stopped

d/Å	60 d	A	A′	B	C
5.57	vs	—	—	—	—
4.00	—	w	w	—	—
3.30	—	—	—	—	s
3.26	sh	vs	vs	—	—
3.20	s	—	vs	vs	s
3.08	vs	—	—	—	—
2.99	—	—	—	—	s
2.90	—	—	—	—	vs
2.83	vw	s	s	—	—
2.77	w	—	s	s	w
2.36	—	w	vw	—	—
2.21	s	—	—	—	m
2.00	—	m	m	—	—
1.95	—	—	m	s	w
1.91	—	—	—	—	s
1.85	m	—	—	—	—
1.84	s	—	—	—	—
1.72	—	m	m	—	—
1.71	—	—	—	—	m
1.67	—	—	m	s	w

A of the process consists of the dehydration of $Nd(OH)_3$ to oxide, whereas the carbonate hydroxide phase formed in the first stages of the aging process would remain unaltered. This conclusion is also supported by the powder diffraction pattern recorded for a sample decomposed at some 20 K above the temperature marked with the arrow A in Figure 2. This diagram, in effect, in addition to the pattern of the carbonate hydroxide phase, shows lines that can be ascribed to cubic neodymia.

The next step of the decomposition process, also consisting of a dehydration reaction, corresponds to the decomposition of the carbonate hydroxide phase, as deduced from the disappearance of the band at 3 425 cm^{-1} (Figure 3, spectrum B). The diffraction pattern of the phase formed at this stage, Table 5, does not show the characteristic lines at 0.326 and 0.283 nm, in accord with the decomposition of the carbonate hydroxide phase.

The third stage of the t.g. diagram in Figure 2 also corresponds to a dehydration process. It can be interpreted as the second step of the decomposition of the carbonate hydroxide-like phase. Presumably, the reaction leads to a monocarbonate dioxide, $Ln_2O_2(CO_3)$, a well known intermediate phase in the decomposition of lanthanide carboxylates,[24,25] carbonates,[26,27] as well as carbonate hydroxides.[26,28] In this respect, it should be mentioned that the evolution of the i.r. spectra on heating parallels that reported [12] for a cubic samaria aged in air, a case in which the formation of a monocarbonate dioxide has also been suggested.

After the last step of the t.g. diagram in Figure 2, that assigned to the decomposition of the monocarbonate dioxide phase to oxide, the powder diffraction pattern show lines corresponding to both hexagonal and cubic neodymia, Table 5. This indicates the occurrence of the well known C to A phase transition in the oxide.[29]

Discussion

In a very recent review [14] we have proposed a classification of the rare-earth-metal sesquioxides based on their behaviour towards atmospheric CO_2 and H_2O, at ordinary temperature and pressure, *i.e.* under the usual storage and manipulation conditions. In accordance with this classification, three groups of oxides, hereafter referred to as I, II, and III, can be distinguished.

In ref. 14 several hexagonal lanthana samples, a commercial hexagonal neodymia, as well as a samaria sample, probably monoclinic,[11,13] were included in group I. Upon exposure to air, these oxides are thoroughly transformed into the corresponding $Ln(OH)_3$. For all of them, carbonation phenomena which affect the bulk have been observed. Nevertheless, no carbonated phase could ever be identified by powder diffraction, which seems to be a characteristic of this group of oxides. Moreover, a lanthana aged in air was treated with flowing CO_2, under normal pressure, in an attempt to increase the carbonation level. This was achieved, but no new lines could be observed in the powder diffraction pattern.[30]

According to ref. 14, the so-called group II includes cubic samaria and europia. The differences in behaviour between the oxides belonging to groups I and II are notable. In the latter case the transformation of the starting oxides is not complete at apparent stabilization. It has also been proposed that aging of the oxides of group II in air leads to the formation of a carbonate hydroxide phase.[12] However, no evidence could be obtained from *X*-ray powder diffraction for the existence of an hydroxide in aged samples of this group of oxides.[12]

Group III, the sesquioxides, which will not be considered further in this work, comprises the heaviest members of the lanthanide series. In particular, oxides of Dy, Ho, and Yb have been suggested to belong to this group.[14]

Regarding the hexagonal and cubic samples of neodymia investigated here, we propose to include them, in groups I and II respectively, of the above classification.

In effect, the results of our study support the existence of very similar behaviour between Nd_2O_3-A samples and the oxides of group I.[8,10,12-14]

The inclusion of Nd_2O_3-C samples in group II deserves further comment. The exposure to air of both the oxides of group II and the cubic neodymia samples leads to the formation of an isostructural crystalline carbonate hydroxide. The difference between the cubic neodymias and the remaining oxides belonging to group II is that, in the former case, the formation of the carbonate hydroxide is followed by hydration of the unreacted oxide to $Nd(OH)_3$, a process which is not observed with cubic samaria and europia.[14]

Our proposal above is mainly based on the i.r. and powder diffraction data, especially the latter. Figure 4 shows the diffraction patterns for cubic Nd_2O_3, Sm_2O_3, and Eu_2O_3, and superimposed upon them, with dotted lines, the patterns of the phases resulting from their exposure to air. In the case of Nd_2O_3 the dotted line actually corresponds to the pattern obtained after the first step of the decomposition of the sample stabilized in air, *i.e.* that reported for A in Table 5. It is obvious from

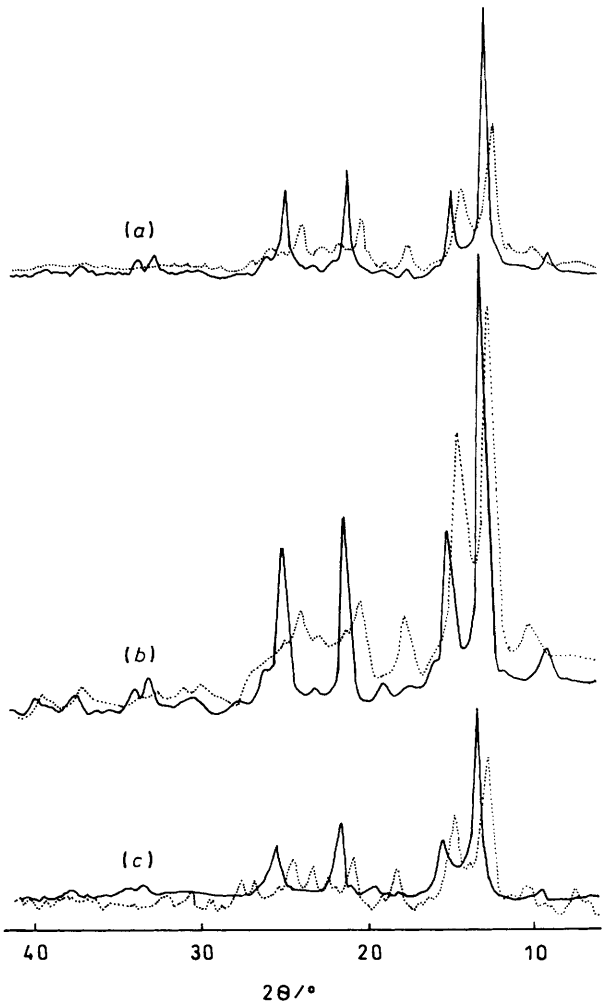

Figure 4. *X*-Ray powder diffraction patterns corresponding to cubic neodymia (*a*), samaria (*b*), and europia (*c*) (full line), as well as to the carbonated phases resulting from their aging in air (dotted lines). The radiation used was Mo-K_α

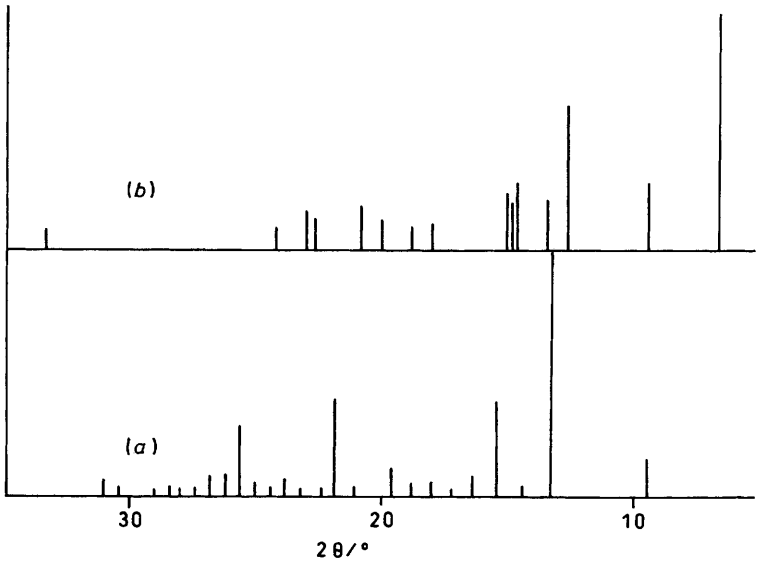

Figure 5. *X*-Ray powder diffraction patterns of cubic Ho_2O_3 (*a*) and monoclinic $Ho_2(OH)_4(CO_3)$ (*b*). The latter is a computer simulation based on the crystallographic data reported in ref. 31. Pattern (*a*) was taken from the ASTM file. Mo-K_α radiation was employed in each case

Figure 4 that the aging of cubic neodymia, samaria, and europia in air leads to the formation of phases the structures of which are very closely related.

In accordance with ref. 31, there are three well known lanthanide carbonate hydroxides: orthorhombic, type A; hexagonal, type B; and monoclinic. The i.r. spectra and powder diffraction diagrams recorded by us do not agree with those reported in the literature for carbonate hydroxides of types A and B.[21,31–34] The structure of the monoclinic $Ho_2(OH)_4(CO_3)$ has recently been reported.[31] From the structural data given, a computer-simulated diffraction pattern for monoclinic holmium carbonate hydroxide has been obtained. This as well as the pattern for cubic Ho_2O_3 is given in Figure 5. When Figures 4 and 5 are compared, it can be concluded that the correlation observed when going from neodymium through europium in Figure 4 fails for holmium. In particular, no diffraction line at around 0.626 nm (6.5° when using Mo-K_α radiation), the most intense in the pattern for the holmium carbonate hydroxide, can be observed in the patterns in Figure 4. This suggests that the phase formed upon exposure of cubic neodymia, samaria, and europia to air does not correspond to any of the three types of lanthanide carbonate hydroxides reported to date. It is obvious, on the other hand, that it does not agree with that formed when oxides belonging to the so-called group I are exposed to air.

As further support to the tentative classification of the rare-earth-metal oxides proposed in ref. 14, the results discussed above show the existence of significant differences in the rates of the aging processes, the nature of the phases formed, as well as in the mechanism of thermal decomposition between the cubic and hexagonal samples of neodymia. These differences are particularly noteworthy in the present case because the oxides belong to a single element. Furthermore, when the nature of the oxides included in groups I and II is analysed, it can be concluded that samples of the same 4*f* element in air behave in a very different way to oxides of unlike lanthanide ions. Such is the case for the samarium oxides,[11–13] and for the neodymium oxides investigated here.

Our results, on the other hand, strongly suggest that the structural nature of the rare-earth-metal sesquioxides may constitute one of the major clues to the observed differences in behaviour. It is worth recalling that the oxides of group II are all cubic, whereas those of group I are hexagonal, except for the samaria sample, which is probably monoclinic.[13] As is well known, however, the hexagonal and monoclinic structures of the lanthanide sesquioxides are closely related to each other,[15] which might justify the observed analogies in their behaviours in air.

From the results in Table 2, some other interesting differences between the cubic and hexagonal neodymia samples can be noted. Thus, the stabilization in air of samples A results in important alterations in both the mean crystallite size and the BET surface area of the oxides. On the contrary, the effect of aging on these properties is much less important in the case of samples C. In other words, the textural modifications induced in the rare-earth-metal oxides by their exposure to air also seem to depend on the structure of the starting oxides. Accordingly, the method proposed in ref. 16 to increase the surface area of lanthana, consisting of subjecting the oxide to successive hydration–dehydration cycles, will probably not work when applied to cubic 4*f* sesquioxides. This procedure is, however, routinely applied to the lanthanide oxides used in catalysis,[35] no matter what the structure.

In conclusion, our results show that the behaviour in air of the rare-earth-metal sesquioxides is much more complex than presumed earlier. The actual nature of the phases formed when these oxides, as is usual, are stored and manipulated in air, is not well known. From our point of view, data like those discussed in this work are considered very valuable, because they can contribute to a better understanding of the reactions in which the lanthanide oxides are involved. In particular, the knowledge of the chemistry in air of the lanthanide oxides may help to improve the synthetic methods currently used to prepare various novel materials[1,2] based on 4*f* oxides.

Acknowledgements

We thank the Comisión Asesora de Investigación Científica y Técnica (CAICYT), for financial support, and Dr. P. Valerga for the computer program used to simulate the diffraction pattern of monoclinic $Ho_2(OH)_4(CO_3)$.

References

1 A. M. Stacy, J. V. Badding, M. J. Geselbrach, W. K. Haw, G. F. Holland, R. L. Hoskins, S. W. Keller, C. F. Millikan, and H. C. Loye, *J. Am. Chem. Soc.*, 1987, **109**, 2528.
2 C. Sudhakar and M. A. Vannice, *Appl. Catal.*, 1985, **14**, 47.
3 M. P. Rosynek, *Catal. Rev. Sci. Eng.*, 1977, **16**, 111.
4 S. Bernal, F. J. Botana, R. García, F. Ramírez, and J. M. Rodríguez-Izquierdo, *Appl. Catal.*, 1986, **21**, 379.
5 S. Bernal, F. J. Botana, R. García, F. Ramírez, and J. M. Rodriguez-Izquierdo, *Appl. Catal.*, 1987, **31**, 267.
6 S. Bernal, F. J. Botana, R. Garcia, F. Ramírez, and J. M. Rodriguez-Izquierdo, *J. Chem. Soc., Faraday Trans. 1*, 1987, 2279.
7 S. Bernal, R. García, J. M. López, and J. M. Rodriguez-Izquierdo, *Collect. Czech. Chem. Commun.*, 1983, **48**, 2205.
8 S. Bernal, F. J. Botana, R. García, and J. M. Rodriguez-Izquierdo, *Thermochim. Acta*, 1983, **66**, 139.
9 R. Alvero. J. A. Odriozola, J. M. Trillo, and S. Bernal, *J. Chem. Soc., Dalton Trans.*, 1984, 87.
10 S. Bernal, J. A. Díaz, R. Garcia, and J. M. Rodriguez-Izquierdo, *J. Mater. Sci.*, 1985, **20**, 537.
11 S. Bernal, F. J. Botana, J. Pintado, R. García, and J. M. Rodriguez-Izquierdo, *J. Less-Common Met.*, 1985, **110**, 433.
12 S. Bernal, F. J. Botana, R. García, J. Pintado, and J. M. Rodríguez-Izquierdo, *Mater. Res. Bull.*, 1987, **22**, 131.
13 S. Bernal, F. J. Botana, R. Garcia, and J. M. Rodriguez-Izquierdo, *Mater. Lett.*, 1987, **6**, 71.
14 S. Bernal, F. J. Botana, R. Garcia, and J. M. Rodriguez-Izquierdo, *Reactiv. Solids*, 1987, **4**, 23.
15 D. Touret and F. Queyroux, *Rev. Chim. Miner.*, 1972, **9**, 883.
16 M. P. Rosynek and D. T. Magnuson, *J. Catal.*, 1977, **46**, 402.
17 H. T. Fullam and F. P. Roberts, report BNWL-1421, Battelle-Northwest, Richland, Washington, D.C., 1970.
18 G. Tosun and H. F. Rase, *Ind. Eng. Chem., Prod. Res. Dev.*, 1972, **11**, 249.
19 A. F. Moskvicheva, G. D. Beregovaya, and B. N. Rybakov, *Russ. J. Inorg. Chem.*, 1971, **16**, 475.
20 M. P. Rosynek and D. T. Magnuson, *J. Catal.*, 1977, **48**, 417.
21 H. Dexpert, E. Antic-Fidancev, J. P. Coutures, and P. Caro, *J. Crystallogr. Spectrosc. Res.*, 1982, **12**, 129.
22 B. I. Swanson, C. Machell, G. W. Beall, and W. D. Milligan, *J. Inorg. Nucl. Chem.*, 1978, **40**, 694.
23 N. V. Zubova, V. M. Makarov, V. D. Nikolskii, P. N. Petrov, E. G. Teterin, and N. T. Chebotarev, *Russ. J. Inorg. Chem.*, 1968, **13**, 7.
24 R. P. Turcotte, J. M. Haschke, M. S. Jenkins, and L. Eyring, *J. Solid State Chem.*, 1970, **2**, 593.
25 I. S. Splygin, V. P. Komarov, and V. B. Lazarev, *J. Therm. Anal.*, 1979, **15**, 215.
26 P. Caro, J. C. Achard, and O. de Pous, *Colloq. Int. CNRS*, 1970, **1**, 285.
27 V. V. Samuskevich, E. A. Prodan, and M. A. Pavlichenko, *Russ. J. Inorg. Chem.*, 1965, **27**, 2525.
28 H. Dexpert, G. Schiffmacher, and P. Caro, *J. Solid State Chem.*, 1975, **15**, 301.
29 M. Foex and J. P. Traverse, *Rev. Hautes Temp. Refract.*, 1966, **3**, 429.
30 S. Bernal, F. J. Botana, R. García, F. Ramírez, and J. M. Rodríguez-Izquierdo, *J. Mater. Sci.*, 1987, **22**, 3793.
31 A. N. Christensen and R. G. Hazell, *Acta Chem. Scand., Ser. A*, 1984, **38**, 157.
32 G. W. Beall, W. O. Milligan, and S. Mroczkowski, *Acta Crystallogr., Sect. B*, 1976, **32**, 3143.
33 J. M. Haschke and L. Eyring, *Inorg. Chem.*, 1971, **10**, 2267.
34 H. Dexpert and P. Caro, *Mater. Res. Bull.*, 1974, **9**, 1577.
35 M. D. Mitchell and M. A. Vannice, *Ind. Eng. Chem., Fundam.*, 1984, **23**, 88.

Received 31*st July* 1987; *Paper* 7/1409